

SPE 12247

Some Observations on Field-Scale Simulation of the In-Situ Combustion Process

by K.H. Coats, *Scientific Software-Intercomp*

Member SPE-AIME

Copyright 1983 Society of Petroleum Engineers of AIME

This paper was presented at the Reservoir Simulation Symposium held in San Francisco, CA, November 15-18, 1983. The material is subject to correction by the author. Permission to copy is restricted to an abstract of not more than 300 words. Write SPE, 6200 North Central Expressway, Drawer 64706, Dallas, Texas 75206 USA. Telex 730989 SPEDAL.

ABSTRACT

This paper describes and illustrates a method for ensuring sustained combustion in coarse-grid, field-scale simulation using a kinetic-based model. For the example problem treated, as in several unreported cases, the method considerably extends the grid block size which can be tolerated without severe grid size effects. The method is applicable only in cases where one accepts the assumption that no free oxygen passes unreacted through the combustion front.

The paper also presents and discusses results of very fine-grid one-dimensional simulations. Comparison of these fine-grid results with coarse-grid 1D results shows, for the particular problem data used, an unexplained, significant increase in amount of oil cracked with grid block size increased over the range of .5 feet to 10 feet.

2D areal, 5-spot pattern simulations show that the 9-point difference scheme very significantly reduces a large grid orientation effect in 5-point simulation of the combustion process.

INTRODUCTION

Several authors¹⁻⁵ have described finite-difference, multidimensional simulation models for the in-situ combustion process. With some oversimplification, each of these models may be denoted as a kinetic-controlled or a reactant-controlled model. A reactant-controlled model assumes that oxygen reacts instantaneously with oil upon contact. A kinetic-controlled model uses Arrhenius type reaction rate expressions for oil oxidation and other reactions. The kinetic-controlled type of model can give results virtually identical to those of the reactant-controlled model if the Arrhenius activation energy in the former is low enough to cause essentially instantaneous consumption of oxygen upon contact with oil.

Crookston et al² described a kinetic-controlled model with reactions accounting for light and heavy oil oxidation, heavy oil cracking and coke oxidation. Youngren's reactant-controlled model³ assumed instantaneous reaction of oxygen with oil in a single oxidation reaction. Coats⁴ described a kinetic-controlled model allowing any number

References and illustrations at end of paper.

of Arrhenius type oxidation and cracking reactions. Hwang et al⁵ described a reactant-controlled model with instantaneous oxidation, as in Youngren's case, and introduced a novel moving-front capability to track the combustion flame front.

Our experience with the kinetic-controlled type of model has been favorable in simulation of laboratory, adiabatic combustion tube tests and in some field-scale cases. However, we have been unable to economically simulate a number of field-scale problems in two or three dimensions. The reason for this inability is that for either sufficiently large block length (in the primary direction of flow) and/or oxidation reaction activation energy, the fire or combustion simply ceases. That is, combustion can be initiated in the air or oxygen injection grid block but, upon burnout of that block, the next block is insufficiently heated to sustain combustion. Hwang et al⁶ noted this effect in their study of sensitivity to a number of combustion problem parameters. The remedy of decreasing the block size can lead to prohibitively large number of blocks and computing time.

The primary purpose of this work was to explore methods of sustaining the combustion in field-scale, kinetic-controlled model simulations while minimizing the effects of spatial truncation error (grid block size). The method described below uses the "Youngren assumption" of instantaneous (reactant-controlled) oil oxidation but retains the kinetic-controlled cracking and coke oxidation reactions. A second purpose of this work was analysis of very fine-grid combustion simulation results and their comparison with coarse-grid results.

The model used in this work is a considerably extended version of a previously described thermal model⁴. While the basic formulation and PVT treatment are unchanged, a large number of features have been added and efficiency has been increased. The additional features pertinent in this work are described by Coats and Ramesh⁷.

The complexity of the combustion process makes generalizations from results for a given data set very difficult. With one exception, the results and fine-grid mechanistic discussions in this paper should be viewed only in the context of the particular data set used. Different data sets can give dramatically different calculated behavior of the combustion process. We attempt to relate

as much insight or understanding as possible regarding the behavior computed for the particular data set used here. We do not claim that this behavior is generally representative of combustion processes.

As an example of this difficulty in generalization, Hwang et al⁶ concluded in their sensitivity study that reactions 2-4 of the four reactions could be eliminated without changing results. While we use the same four reactions here, (with different parameters), our results are dramatically changed by dropping reactions 2-4.

The one exception mentioned above is that the method described below for ensuring sustained combustion has worked well on a number of combustion data sets to date. With its adjustable parameter, we feel that it may serve its purpose well for a wide range of combustion problems.

THE ACTIVATION TEMPERATURE CONCEPT

Kinetic models previously described^{2,4} utilize an Arrhenius term of the type $e^{-E/RT}$ in the reaction rate expressions for oil oxidation, cracking and coke oxidation. At low temperature, this term can be very small. In computations with sufficiently large activation energy E or grid block size it can be so small that a grid block adjacent to a burned-out block will not ignite. Free oxygen then flows through that block and others downstream and the combustion simulation fails.

For most combustion problems within our experience, the heat released by the heavy oil oxidation reaction is the source of the heat necessary to raise grid block temperature T and the value of $e^{-E/RT}$ sufficiently to initiate or continue the combustion. The temperature rise caused by that heat release in turn leads to cracking and subsequent coke oxidation. That is, in a sense heavy oil oxidation is a "cause" and cracking and coke oxidation are "effects" in the combustion process. This statement is a generality with exceptions. That is, activation energy can be assigned sufficiently high and low values for oil oxidation and cracking/coke oxidation, respectively, such that cracking and oxidation of the resulting coke cause heat generation and oil oxidation is then effected. Hwang et al⁷ demonstrate this dependence of primary heat source upon activation energies.

In this work we used an activation temperature, T_{ACT} , in conjunction with Arrhenius terms of e^{-E/RT^*} in the heavy and light oil oxidation reactions, where

$$T^* = T_{ACT} \text{ if } T \leq T_{ACT}$$

$$T^* = T \text{ if } T \geq T_{ACT}$$

This has no effect on all the grid blocks downstream of the combustion front because oil oxidation rate is zero there due to the absence of oxygen. However, as a grid block adjacent to and downstream of a frontal block nearing burnout experiences oxygen inflow, it will consume the oxygen at a rate proportioned to $e^{-E/RT_{ACT}}$, if the block temperature is less than T_{ACT} when oxygen inflow begins. This value of $e^{-E/RT_{ACT}}$ may be much larger than $e^{-E/RT}$ when this oxygen inflow begins. The value of T_{ACT} is chosen sufficiently large that essentially all oxygen is consumed by the heavy oil oxidation reaction. The value is a constant for a given run, independent of spatial position and time.

We have used a value of 400°F (860°R) for T_{ACT} in a number of combustion problems where the activation energy for the heavy oil oxidation reaction ranged from 17,000 to 20,000 cal/g mole. T_{ACT} should be higher for larger and lower for smaller activation energies. The procedure followed for estimating T_{ACT} is as follows. A one-dimensional problem is simulated, using an air or oxygen flux and Δx grid block size of interest in the study. A first run is performed with $T_{ACT} = 0$. If, with or without artificial initiation of combustion in the first block, combustion is sustained in this run with negligible passage of unreacted oxygen through the flame front, then the T_{ACT} feature is unnecessary. If, however, the calculated combustion ceases or substantial free oxygen passes unreacted through the front, the 1D run is repeated with $T_{ACT} =$ (say) 760°R, 860°R, etc, until essentially zero oxygen mol fractions are computed in blocks downstream of the frontal block. These 1D runs need not be continued past the burnout of the first few grid blocks and are therefore very inexpensive.

Other, simpler methods of forcing instantaneous oxygen reaction with oil are the use of artificially low activation energy (e.g. $E = 4000$ cal/g-mol) or using $E = 0$ and increasing the frequency factor (rate constant) A_f for the oil oxidation reactions. We prefer the T_{ACT} method because it automatically inactivates itself when temperature rises above T_{ACT} . That is, above T_{ACT} all reactions compete for oxygen in accordance with the originally specified kinetic parameters. Relative rates of cracking and oxidation of heavy oil, light oil and coke are unaffected by the method at temperature above T_{ACT} .

As stated by Youngren³, the forcing of instantaneous oxygen consumption in a model requires acceptance of the assumption that combustion is sustained and no significant amount of unreacted oxygen will pass through the front and be produced. He also states such a model will not apply to wet partially quenched combustion. We feel some degree of quenching should be compatible in a model with the Youngren assumption but we have not studied that question.

EXAMPLE PROBLEM DATA

Table 1 lists reservoir, fluid and reaction kinetic data used in this work. The six components are H₂O, HO, CON₂, COKE, O₂ and LO, where HO and LO are heavy and light oil components with molecular weights of 350 and 142, respectively. The original reservoir oil phase is 100% HO with viscosities of 272 cp at the initial formation temperature of 100°F and 1.07 cp at 544.4°F. The light oil (LO) is assigned a K-value behavior similar to that of decane. The component CON₂ is used to represent both nitrogen in injected air and CO/CO₂ combustion products. Solubilities of CON₂ and O₂ in oil and water are ignored.

The reaction kinetic data are nearly identical to those given by Crookston et al² for their example problem. The four reactions are HO oxidation, LO oxidation, cracking and coke oxidation, respectively, with oil oxidation heats of reaction equal to 20,000 Btu/lbm.

Relative permeability data utilize temperature independent values of $S_{wc} = .2$, $S_{orw} = .3$, $S_{org} = .09$, $S_{gc} = .05$ and $k_{rwro} = .25$. Initial fluid saturations are $S_{wc} = .3$, $S_{oi} = .55$ and $S_{gi} = .15$ so that water and gas are both mobile at initial conditions.

Air is injected at a constant rate of 190.48 MSCF/D with the production well at $x = L = 100$ feet on

deliverability at 150 psia with a productivity index of 945 RB-cp/day-psi. This injection rate corresponds to an air flux of 90.7 SCF/day-sq. ft. or an oxygen flux of 19 SCF/day-sq. ft., based on total reservoir cross-sectional area normal to flow (product of width and gross thickness).

Original-oil-in-place (OOIP) is 4464 STB for the 100' length used in one-dimensional runs and 8928 STB for the 200' length used in the two-dimensional cross-sectional runs. The OOIP is 48,613 STB for the 1/8, 20-acre 5-spot pattern runs.

ONE-DIMENSIONAL RUN RESULTS

One-dimensional Runs 1-4, were performed with zero heat loss as follows:

RUN	L	N_x	Δx	TACT
1	100	10	10	0
1A	100	10	10	400
2	100	40	2.5	0
3	20	40	.5	0
4	100	47	1.25-10	0

Run 4 used forty 1.25', two 2.5', one 5' and four 10' grid blocks. For Runs 1 and 2-4, combustion was initiated by initializing the first grid block with $S_{wi} = 0$, $S_{oi} = .55$, $S_{gi} = .45$, $T_1 = 550^\circ\text{F}$; also, heat was injected into the first block at 550°F for a few days until combustion resulted in temperature increase.

Figure 1 shows the calculated mol fraction of oxygen in the effluent (produced) gas phase for Runs 1-3 and 1A. In Run 1 with $\Delta x = 10'$, the combustion barely continued with produced oxygen peaks corresponding to time periods between completion of combustion in one block and vigorous ignition in the next block. As Δx was decreased from 10' to 2.5' and .5' in Runs 2 and 3, the produced oxygen tended toward zero, indicating a reactant-controlled process.

An oxygen utilization efficiency is defined as 1-(cumulative free oxygen production)/(cumulative oxygen injection) at a time corresponding to the occurrence of peak temperature in the last (producing) grid block. For Runs 1, 2 and 3, the efficiencies were 78.4, 87.4 and 95.6%, respectively. The efficiency of Run 1A using $\Delta x = 10'$ with TACT = 400°F was 97.1%.

Figure 2 shows calculated oil recovery (% of OOIP) vs. time for Runs 1-3. These recovery curves are considered as basically identical subject to the following observations. For Runs 1, 2 and 3, the first grid block was initialized with zero S_w and a 550°F temperature and heat was injected, as described above. This accelerated the combustion in the first grid block, compared to Run 1A which had no variation in initial temperature or saturations. Thus the recovery curves for Runs 1-3 start above that of Run 1A and continue higher. Run 3 is not "scaled" in that it represents only the first 20 feet of the 100 ft. length of the other runs. The second-order heat conduction effect is not scaled and the heat conduction zone occupies a much larger fraction of total length in Run 3 than in the other runs. Run 3 results are valid for comparison purposes only for a period of time before high temperatures in the conduction zone (ahead of the combustion front) appear at $x = 20$ feet. For comparison purposes, Run 3 results on Figure 2 are plotted vs. time $t^* = 5t$ where t is actual run time.

The above-claimed close agreement of the Figure 2 recovery curves is deceptive in a sense briefly mentioned here and discussed more fully below. The cracking stoichiometry and the stock tank densities and molecular weights of heavy and light oils result in volumetric equivalence of stock tank oil from the cracking reaction. That is, one STB of heavy oil yields essentially one STB of light oil in the cracking reactor 3. Table 2 shows that with $\Delta x = 10'$ (Runs 1 or 1A), the STB of heavy oil cracked is at least twice as large as that calculated for $\Delta x = 2.5'$ (Run 2). Stated in other terms, light oil is 18.5% of total oil recovery with $\Delta x = 10'$ and only 8.3% with $\Delta x = 2.5'$. The amount of heavy oil cracked seems sensitive to block size while the amount burned is relatively insensitive.

Figure 3 shows calculated peak temperature vs. distance for Runs 1-3. The peak temperatures for $\Delta x = 2.5'$ and .5' (Runs 2 and 3) agree very well, indicating that a grid dimension of about 1 ft. is sufficiently small to eliminate spatial truncation error for this particular data set. For $\Delta x = 10$ ft., the use of TACT = 400°F has little effect on calculated peak temperature. Also, the peak temperatures for $\Delta x = 10$ ft. agree reasonably well with those calculated for $\Delta x = 2.5$ and .5 ft.

The general trend of peak temperature decline with distance travelled is attributed to the distillation/displacement effect, discussed below. The increase in calculated peak temperature near $x = L$ (for small Δx) is believed due to the loss of the heat conduction effect as the combustion front nears $x = L$.

In all these ID runs, negligible light oil was burned, indicating that the light oil oxidation reaction can be omitted for these particular problem data.

These 1D runs were repeated with heat loss. For all cases, heat loss resulted in peak temperatures roughly 100°F lower and ultimate oil recoveries of 84-87% compared to the 91-93% with no heat loss. For Run 1A, heat loss increased breakthrough time (time of temperature peak and zero oil saturation in the producing block) from 181 days to 273 days. Thus, for these problem data, heat loss increases air requirement by 50% and reduces ultimate oil recovery by 7%. For Runs 1, 1A and 2, the heat loss at breakthrough was 62-65% of the total heat of reaction.

In Runs 1 and 1A with no heat loss, the HO burned values were 300 and 360 STB, respectively. Heat loss increased these values to 562 and 652, respectively, which accounts for the lower recoveries with heat loss. The heat loss slightly lowered the HO cracked in those runs from 775 STB to 617 STB. For Run 2, the amounts of HO burned and cracked were 387 and 337 STB, respectively, with no heat loss and 584 and 280 STB, respectively, with heat loss.

We define H_{41} as the ratio of coke oxidation heat of reaction to HO oxidation heat of reaction at breakthrough time, expressed as a percentage. For the 10' Δx Runs 1 and 1A, H_{41} was about 16% and 38% with and without heat loss, respectively. For the 2.5' Δx Run 2, H_{41} was 8 and 14%, respectively. Thus, most of the heat of reaction for this particular problem is generated by HO oxidation as opposed to coke oxidation.

Run 1 was performed with no alteration of the kinetic data and the amounts of HO burned and cracked, for zero heat loss, were 300 and 779 STB, respectively. A Run 1B with oil oxidation activation energy lowered to 3000 cal/g-mol gave 434 and 700 STB of HO burned and

cracked. The corresponding Run 1A ($T_{ACT} = 400^{\circ}F$) HO amounts of 360 and 770 STB are somewhat closer to the "unaltered" Run 1 results than are the Run 1B values.

With heat loss included, the STB of HO burned and cracked were respectively 562 and 620 for Run 1, 652 and 615 for Run 1A, and 711 and 542 for Run 1B. Again, the use of $T_{ACT} = 400^{\circ}F$ gives results somewhat closer to the unaltered (Run 1) values than does use of a lowered oxidation activation energy. With other kinetic data sets we have noted a more pronounced preference in this respect for use of T_{ACT} rather than a lowered activation energy.

2D CROSS-SECTIONAL RESULTS

Cross-sectional runs were performed with the following changes in Table 1 data. The formation thickness was divided into three layers, each 7 feet thick, with vertical permeability of 400 md. Reservoir length was increased from 100 to 200 feet and initial water, oil and gas saturations were .4, .55 and .05, respectively. Runs 5, 6 and 7 were made with 5 x 3, 10 x 3 and 20 x 3 x-z grids, or Δx values of 40, 20 and 10 feet, respectively. Heat loss was accounted for in accordance with the overburden conductivity and specific heat data of Table 1. Air was injected at 190.48 MSCF/D into layer 3 at $x = 0$ and production was specified at $x = 200$ feet from layer 3 on deliverability at 150 psia with a productivity index of 80 RB-cp/day-psi.

All runs were made with $T_{ACT} = 400^{\circ}F$. A 5 x 3 run with $T_{ACT} = 0$ resulted in an upward burn from layer 3 to the top layer above the injector and then essentially a cessation of combustion. After 600 days of injection, 15,000 MSCF of free oxygen had been produced compared with 24,000 MSCF of oxygen injected.

Figure 4 shows that the x-direction grid block dimension, within the range of 10-40 feet, has little effect on calculated oil recovery. The calculations showed a strong gravity override as indicated by the oil saturation and temperature profiles shown on Figure 5 for the 20 x 3 Run 7 at 400 days. Peak temperatures (in blocks other than those near $x = 0$ and $x = 200$ feet) ranged from about 420 $^{\circ}F$ in the 5 x 3 Run 5 to about 600 $^{\circ}F$ in the 20 x 3 Run 7. Thus while the Δx value significantly affected peak temperature, it did not seem to materially affect calculated oil recovery. The one-dimensional run with heat loss and $\Delta x = 10'$ (Run 1A with heat loss) gave a peak temperature nearly constant at about 600 $^{\circ}F$.

Table 3 compares heavy and light oil burned, cracked and recovered, and injector/producer peak temperatures and times for the three runs. In all cases the heat loss was about 70% of the total heat of reactions. Table 3 shows that the amounts of heavy oil burned and cracked and recoveries of light and heavy oil are relatively insensitive to the Δx grid dimension over this 10'-40' range. Light oil represents about 25% of total oil recovery.

Breakthrough time, or time of the production block temperature peak, is about the same, 514-500 days, for the 10 x 3 and 20 x 3 runs and is 560 days for the 5 x 3 run. The amount of light oil burned is small and decreases with decreasing Δx , indicating, as in the one-dimensional cases, that the light oil oxidation reaction can be ignored. This is in agreement with one of the conclusions reached by Hwang et al⁶.

Calculated free oxygen production for these cross-

sectional runs was essentially zero up to the time of the production block temperature peak. Free oxygen production increased sharply immediately following that peak in all cases.

5-SPOT PATTERN RESULTS

Runs 8-11 represent 1/8 of a 20-acre 5-spot pattern with 2D areal grids. Runs 8 and 9 used diagonal 5 x 5 and parallel 7 x 4 grids, respectively. The square grid block dimension (Δx) is about equal for these two grids, 116.7' for the 5 x 5 grid and 110' for the 7 x 4 grid. Runs 10 and 11 used diagonal 8 x 8 and parallel 11 x 6 grids, respectively. The square grid block size (Δx) is 66.7' for the 8 x 8 grid and 66' for the 11 x 6 grid. The terms "parallel" and "diagonal" were introduced by Todd et al⁸ in their discussion of grid orientation effects. The four grids just mentioned are shown and discussed in detail by Coats and Ramesh⁷.

Agreement between Runs 8 and 9 and between Runs 10 and 11 should be good except for grid orientation effects. Agreement between Runs 8 and 10 and between Runs 9 and 11 should be good except for grid size effects (spatial truncation error).

Runs 8-11 used the 9-point difference scheme described by Yanosik and McCracken⁹. A companion set of Runs (8A-11A) were made using the conventional 5-point difference scheme. All data, including heat loss parameters, are identical to those given in Table 1 except for the reservoir dimensions (1/8 20-acre 5-spot) and the injection/production conditions. The air injection rate of 190.48 MSCF/D for the 1/8 element corresponds to a total well injection rate of 1524 MSCF/D. Since the average width of 1/8 of a 20-acre 5-spot is 165 feet, the average air flux for these pattern runs is 190.48/(165 x 21) or 55 SCF/day-sq.ft. The corresponding average oxygen flux is 11.54 SCF/day-sq. ft. This flux is about 40% less than that of the previous 1D and 2D cross-sectional Runs 1-7. Production was on deliverability at 150 psia with productivity indices reflecting the pattern, grid orientation, difference scheme and number of grid blocks⁷. For example, the PI was 9.864 RB-cp/day-psi (for 1/8 of a well) for the 8 x 8, diagonal grid with the 9-point difference scheme.

All runs discussed here were made using $T_{ACT} = 400^{\circ}F$. Combustion was not sustained at these very large grid block sizes ($\Delta x = 66'$ -116') with $T_{ACT} = 0$.

Figure 6 shows a large grid orientation effect when the 5-point difference scheme was used. The 5-point, 8 x 8 diagonal Run 10A and 11 x 6 parallel Run 11A oil recovery curves differ greatly. We define "breakthrough" time as the time of peak temperature and zero oil saturation occurrence in the producing grid block. For the 5-point Runs 10A and 11A, calculated breakthrough times were 4,190 and 2,916 days, respectively.

Figure 6 shows that the 9-point difference scheme very significantly reduces the grid orientation effect. The oil recovery curves for diagonal and parallel Runs 10 and 11 agree well with calculated breakthrough times of 3,000 and 2,785 days, respectively. Comparison of the 7 x 4 Run 9 ($\Delta x = 110'$) and 11 x 6 Run 11 ($\Delta x = 66'$) recovery curves shows a moderate grid size effect. Calculated recovery is somewhat lower for the finer grid (Run 11).

Table 4 reports, for Runs 8-11, oil recovered, burned and cracked and injector/producer peak temperatures and

breakthrough times. Heat loss as a percentage of total heat of reaction was nearly constant for all runs with a range from a low of 77.5% (Run 10) to a high of 78.4% (Run 9). The calculated recoveries of heavy oil, light oil and amounts of heavy oil burned and cracked differ moderately among the runs but show no obvious correlation with grid orientation or grid size. The light oil recoveries as percentages of total oil recovery were 38.2, 42.3, 40 and 46.4% for Runs 8-11, respectively. Breakthrough time was about 3,000 days for all runs except the 7 x 4 Run 9 (3,840 days).

Table 4 shows more significance of the light oil oxidation reaction in these 2D areal runs than in the previously described 1D and 2D cross-sectional runs.

For the 8 x 8 Run 10, peak temperatures were fairly uniform and about 450-475°F for most blocks removed from the wells. For the 11 x 6 Run 11, peak temperatures were roughly 550°F along the injector-producer row of blocks. However, the peak temperatures fell to 410-460°F in the next row, were 350-390°F or less in the third row and less than 350°F in rows further removed from the injector-producer row.

Peak temperatures in grid blocks removed from the wells were about 100°F lower in the 5 x 5 Run 8 than in the 8 x 8 Run 10. In the 7 x 4 Run 9, peak temperatures in the first (injector-producer) and next rows were about 100°F less than in the 11 x 6 Run 11.

COMPARISON OF 1D FINE-GRID AND COARSE-GRID RESULTS

Most of the results described above relate to calculations using grid block dimensions very much larger than the probable width or thickness of the flame front. This front in fact might be considered a plane of zero thickness. Here, then, we present profiles (variable vs. distance plots) generated for fine 1D grid spacings and compare these profiles and other results with coarse-grid 1D results.

Figure 7 shows early-time profiles for 1D Run 4, which used forty 1.25' grid blocks in the first 50 feet of the total 100 feet of reservoir length. The combustion front is at 4 feet with temperature peaking at 706°F at that position (in the 4th grid block). These first 4 feet are referred to as the "burned zone", a zone of zero liquid saturation and 100% gas saturation. Immediately ahead or downstream of the burned zone is a "vaporization zone" with a low, nearly constant oil saturation. In this vaporization zone (of about 4 feet) light oil is being vaporized out of the oil phase and liquid H₂O appears to be completely vaporized, due to the high temperatures resulting from heat conduction immediately downstream of the combustion front. Light oil mol fraction (in the oil phase) peaks sharply at a high value immediately at the downstream edge of this vaporization zone. This sharp condensation peak of light oil in the oil phase occurs at a temperature of about 300°F. Temperature falls very sharply from 706°F at the combustion front to 300°F at a position 1-2 feet ahead of the vaporization zone. Downstream of the vaporization zone, a water-bank zone appears, immediately followed by a much longer oil bank zone.

The oil bank consists of dead oil at original reservoir temperature. Light oil mol fraction is zero in the oil bank; light oil can penetrate the oil bank zone only by dispersion (numerical or physical dispersion/fingering). With fine grids the numerical dispersion is small; physical dispersion,

if modelled, would result in a minor dilution (at the upstream edge) of the overall oil bank length. One might argue that light (low viscosity) oil would tend to unstably finger into/through the heavy (viscous) oil. While there is justification for the claim, a treatment of this fingering phenomenon is beyond the scope of this work. We ignore the fingering effects but do not deny them.

In the cold (original reservoir temperature) oil bank zone, the viscous oil drives water saturation down toward irreducible saturation (.2) and drives gas saturation down toward critical (and residual) saturation (.05). For the data used here, water relative permeability is very low between S_{wi} (.3) and S_{wir} (.2). If k_{rw} were larger in this range, the oil bank would drive S_w down to nearly .2. In any event, the oil bank zone is a zone of very low total mobility; oil mobility is low due to high oil viscosity and water and gas mobilities are low because the viscous oil displaces them down to very low relative permeabilities. The result is a "pressure barrier" or "plugging" effect - a tendency for a large pressure drop to occur from the upstream to downstream edges of the oil bank zone. This effect is small for the moderate heavy oil viscosity (272 CP), reservoir permeability, length and injection rates used here. In cases of heavier oil, lower permeability, etc., this effect can be severe and cause inability to sustain desired injection rates, as noted by Hwang et al⁶. For this Run 4, the upstream edge of the oil bank arrived at $x = L$ (= 100 ft.) at about 110 days. The injection grid block pressure peaked at 355 psia at 36 days and fell continuously to 167 psia at 110 days with the producing block never exceeding 165 psia.

The oil bank zone is essentially a zone of water and gas displacement by heavy oil. Downstream of the oil bank is a zone of gas displacement by water with oil saturation essentially unchanged from its original value.

Figure 8 shows profiles for 1D Runs 2 ($\Delta x = 2.5'$) and 3 ($\Delta x = .5'$, $L = 20'$). The fine-grid Run 3 shows zones near the combustion front more clearly than does Figure 7. We will first discuss the fine-grid ($\Delta x = .5'$, dotted line) results shown in Figure 8 at time = 23 days. Temperature is peaking at 660°F in the 20th grid block at $x = 10$ feet which is the position of the combustion front and length of the burned zone (Zone 1).

Zone 2 shown on Figure 8 is the vaporization zone, about 4 feet long, and can be divided into a 3-ft. zone 2A in which both light oil and all liquid H₂O have been vaporized and a 1-ft. Zone 2B where light oil is essentially vaporized but liquid H₂O remains. The light oil component condenses with a very sharp peak mol fraction of .83 at the downstream edge of the vaporization zone. The vaporization zone contains a constant, heavy (distilled) oil saturation of .07 and this is the "fuel" which the advancing combustion front encounters. For the kinetic reaction data used here, coke saturation in this vaporization Zone 2 is essentially zero.

Downstream of the vaporization Zone 2 is the "water-bank" Zone 3. Temperature and light oil mol fraction fall toward T_i and zero, respectively, in this zone. Downstream of the water-bank Zone 3 is the heavy oil bank zone, shown and discussed above in connection with Figure 7. The oil bank has already been produced out of the 20 ft. length for Run 3 at 23 days.

The solid line profiles of Figure 8 show the masking or smearing effect produced by increasing Δx from .5' in Run 3 to 2.5' in Run 2. Oil saturation is no longer constant in the vaporization zone and the light oil condensation peak

is lower and much less sharply defined. This peak light oil mol fraction is noted by an asterisk on Figure 8 because of its importance in the simulated combustion process. Again, as noted previously, we avoid the question of whether such a sharp peak would physically exist, considering fingering in a light oil/viscous oil miscible displacement.

This peak, condensed light oil mol fraction tends to reduce in two ways the fuel available for or encountered by the combustion front. First, a high LO mol fraction reduces the oil phase viscosity which, in turn, enhances the displacement of oil by water, ahead of the vaporization Zone 2, to low saturations. Second, the higher this peak LO mol fraction, the greater will be the oil shrinkage or saturation decline at the leading edge of the vaporization zone (where high temperatures ahead of the combustion front distill the LO). We will refer to these effects of high peak LO mol fraction as the distillation/displacement, or simply distillation effect.

In general, increasing grid size, Δx , decreases the calculated value of this peak LO mol fraction, x_{LO} . Figure 9 shows x_{LO} vs. distance calculated for grid blocks of .5, 1.25, 2.5 and 10 feet. A value of (peak) $x_{LO} = .83-.84$ is reached using blocks of .5' and 1.25' and, with some delay, for the 2.5' block. However, the 10' block gives substantially lower peak values.

The effect of this lower peak LO mol fraction with larger block size should be an increase in oil saturation encountered by the combustion front and a corresponding increase in combustion front temperature. There are other effects of increased block size, of course, and they may tend to decrease the grid blocks' computed peak temperatures as grid size is increased. While this study has not addressed that question, any such tendency might be partially offset by a lower peak x_{LO} increasing fuel and peak temperature as grid size is increased. We note in this connection that Figure 3 shows a somewhat higher peak temperature for a 10' block than for 2.5' and .5' blocks.

There is a very significant effect of grid size, in the 2.5'-10' range, on the calculated amount of heavy oil cracked. Figures 10 and 11 show cumulative heavy oil burned and cracked, mass/unit bulk volume, vs. distance for grid block sizes of .5', 2.5' and 10'. These figures show that the .5' and 2.5' block sizes agree rather well with burned and (large-distance) cracked HO values of about 3.3 and 1-1.5 lbm/cu. ft., respectively. The 10' block size gives somewhat lower burned values of about 2.8 lbm/cu. ft. But Figure 11* shows that the 10' block gives much higher cracked values, declining with distance from about 8 to 3 lbm/cu. ft.

Our work to date has yielded no explanation for this significant increase in HO cracked with an increase from 2.5' to 10' block size. As shown in Table 3, the 2D cross-sectional runs did not show a trend of increased cracking with x block size increasing from 10' to 20' to 40'. Also, Table 4 shows no increase in cracking as Δx is increased from 66' to 110' in the 2D areal 5-spot runs.

The simple remedy of lowering the cracking reaction level in the 1D 10' block run does not satisfactorily rectify the disparity in cracking levels of the 2.5' and 10' 1D runs.

* If Figure 11 results were plotted vs. distance rather than x/L , the .5' Run 3 results would fall to the left of the 2.5' Run 2 results.

Repeating Run 2 (2.5' block) with all reactions but HO oxidation eliminated resulted in peak temperatures over 2,200°F and a combustion front velocity three times lower than that of Run 2.

SUMMARY

A method is described for sustaining combustion in kinetic-based model simulations using relatively coarse grids. Use of the method requires the Youngren assumption of instantaneous oxygen consumption - i.e. the assumption that negligible amounts of oxygen pass unreacted through the combustion front. The method alters the relative rates of oil vs. coke oxidation reactions below a specified temperature (T_{ACT}). However, it automatically inactivates itself above T_{ACT} and all reaction rates obey user-specified kinetic data above that temperature.

Our experience with a number of kinetic data sets indicates that the method results in moderate to minor alterations of calculated oil cracked vs. oil burned and only moderate grid size sensitivity in the range of "coarse" grid spacings. Cross-sectional, example problem results using the method show a decline in calculated peak temperatures with Δx increasing from 10 to 20 to 40 feet. However, the amounts of light and heavy oil burned, cracked and recovered are nearly constant over this grid size range. Produced and reacted amounts of oil for a 20-acre 5-spot pattern agree well when calculated using 66' square blocks and 110' square blocks. Again, however, the larger grid resulted in somewhat lower calculated peak temperatures.

Fine-grid, one-dimensional results using $\Delta x = .5'$ exhibit a number of zones, including a very short, fuel-containing vaporization zone immediately downstream of the combustion front. Comparison of fine-grid ($\Delta x \leq 2'$) with coarse-grid ($\Delta x \geq 10'$) 1D results shows an unexplained doubling of the calculated oil cracked. This sensitivity of amount of oil cracked to grid size did not seem to occur at larger grid sizes in 2D cross-sectional and areal pattern runs.

2D areal calculations for a 20-acre 5-spot showed a strong grid orientation effect when the 5-point difference scheme was used. The 9-point scheme very significantly reduced this grid orientation effect.

NOMENCLATURE

A_r	reaction rate constant for reaction r
c_i	compressibility of component i, psi ⁻¹
C_{pi}	specific heat of component i, Btu/lb-°F
E_r	activation energy for reaction r, cal/g-mol
HO	heavy oil component
H_r	heat of reaction of reaction r, Btu/lb-mol of first reactant
k_h	horizontal permeability, md
k_v	vertical permeability, md
K_i	K-value for component i, y_i/x_i
k_{rwro}	relative permeability to water at residual oil
k_{rocv}	relative permeability to oil at connate water
k_{rgro}	relative permeability to gas at residual oil
k_{rw}	relative permeability to water

LO	light oil component
L	reservoir length, feet
M_f	rock heat capacity, Btu/cu.ft. rock- $^{\circ}$ F
M_i	molecular weight of component i
OOIP	original-oil-in-place, STB
p	pressure, psia
P_i	initial reservoir pressure, psia
P_{ci}	critical pressure of component i, psia
R	universal gas law constant
S_w	water saturation
S_o	oil saturation
S_g	gas saturation
S_{wi}, S_{oi}, S_{gi}	initial saturations
T_{ci}	critical temperature of component i, $^{\circ}$ R
T	temperature, $^{\circ}$ R (unless noted otherwise)
T_i	initial reservoir temperature
T_{PEAK}	peak temperature in a grid block
v_o	specific volume of oil phase, cu.ft./lb.mol
v_{io}^o	specific volume of component i in the oil phase at 14.7 psia, 60 $^{\circ}$ F, cu.ft./mol
x_{LO}	mol fraction of light oil in the oil phase
Δx	x-direction grid block length, feet
x	distance, feet
x_{io}	mole fraction of component i in oil
x_{ig}	mole fraction of component i in gas
y_{O_2}	mole fraction oxygen in the gas phase

Greek

β_i	thermal expansion coefficient for component i, 1/ $^{\circ}$ F
λ	thermal conductivity, Btu/day- $^{\circ}$ F-ft.
$\rho_{OST,i}$	density of component i in stock tank oil, lbs/cu.ft. ($\rho_{OST,i} = M_i/v_{io}^o$)
μ_o	oil phase viscosity, cp
μ_g	gas phase viscosity, cp
μ_{io}	partial viscosity of component i in oil, cp
μ_{ig}	partial viscosity of component i in gas, cp

REFERENCES

1. Ali, F.S.M.: "Multiphase, Multidimensional Simulation of In-Situ Combustion," paper SPE 6896 presented at SPE 52nd Annual Technical Conference and Exhibition, Denver, Oct. 9-12, 1977.
2. Crookston, H.B., Culham, W.E., and Chen, W.H.: "Numerical Simulation Model for Thermal Recovery Processes," Soc. Pet. Eng. J. (Feb. 1979), 37-58; Trans., AIME, 267.
3. Youngren, G.K.: "Development and Application of an In-Situ Combustion Reservoir Simulator," Soc. Pet. Eng. J. (Feb. 1980), 39-51.

4. Coats, K.H.: "In-Situ Combustion Model," Soc. Pet. Eng. J. (Dec. 1980), 533-554, Trans. AIME, 269.
5. Hwang, M.K., Jines, W.R., and Odeh, A.S.: "An In-Situ Combustion Process Simulator With a Moving Front Presentation," Soc. Pet. Eng. J. (April 1982), 271-279; Trans. AIME, 273.
6. Anis, M., Hwang, M.K., and Odeh, A.S.: "A Sensitivity Study of the Effects of Parameters on Results From an In-Situ Combustion Simulator," Soc. Pet. Eng. J. (April 1983), 259-264.
7. Coats, K.H., and Ramesh, A.B.: "Effects of Grid Type and Difference Scheme on Pattern Steamflood Results", SPE Paper 10079 presented at the 57th SPE Annual Fall Meeting, New Orleans, La., Sept. 26-29, 1982.
8. Todd, M.R., O'Dell, P.M., and Hirasaki, G.J.: "Methods for Increased Accuracy in Numerical Reservoir Simulators," Soc. Pet. Eng. J. (Dec. 1972), 515-530; Trans., AIME, 253.
9. Yanosik, J.L., and McCracken, T.A.: "A Nine-Point, Finite-Difference Reservoir Simulator for Realistic Prediction of Adverse Mobility Ratio Displacements," Soc. Pet. Eng. J. (Aug. 1979), 253-262; Trans., AIME, 267.

TABLE 1

EXAMPLE PROBLEM DATA

Reservoir length, feet	100	Oil Phase Density Data
Reservoir width, feet	100	$v_o = \sum_{i=1}^6 x_{io} v_{io}$
Reservoir thickness, feet	21	$v_{io} = v_{io}^o (1 - c_i(p - 14.7)) \cdot (1 + \beta_i(T - 520))$
k_{h1} , md	2000	$v_{2o}^o = 6.195$
k_{v1} , md	400	$v_{6o}^o = 3.117$
Porosity	.22	coke density = 80 lbs/cu.ft.
Rock heat capacity M_f	35	
Thermal conductivity, λ	38.4	
Overburden thermal conductivity, λ	38.4	
Overburden heat capacity, M_f	35	
Formation compressibility, 1/psi	10^{-5}	
T_i , °F	100	
P_i , psia	150	

Initial S_w, S_o, S_g .3, .55, .15
 Initial mol fractions $X_1 = X_2 = X_4 = 1.0, X_3 = X_5 = X_6 = 0$

i	COMPONENT	M_i	P_{ci}	T_{ci}	c_i	β_i	C_{pi}	$\rho_{ost,i}$
1	H2O	18						
2	HO	350			10^{-3}	.00038	.5	56.5
3	CON2	44	1073	547.7			.25	
4	COKE	13.2					.3	
5	O2	32	730	277.9			.24	
6	LO	142	305.8	1111.7	10^{-3}	.00038	.5	45.55

VISCOSITY DATA

$\mu_o = \frac{6}{\pi} \sum_{i=1}^6 \mu_{io} x_{io}$	T (°F)	μ_{2o}	μ_{6o}	μ_{3g}	μ_{5g}	μ_{6g}
$\mu_g = \frac{6}{\pi} \sum_{i=1}^6 \mu_{ig} x_{ig}$	100	272	.80	.018	.021	.018
$\mu_{io} = e^{A_{io}} T^{B_{io}} - 1.0$	600	.83	.04	.028	.034	.028
$\mu_{ig} = A_{ig} T^{B_{ig}}$						

K-value data

$K_6 = x_{6g}/x_{6o} = (1280 + 216,600/p) e^{-8394/T}$

Capillary pressure = 0.

Relative Permeability Data*

$S_{wir} = .2$	$k_{rwo} = .25$
$S_{orw} = .3$	$k_{rocw} = 1.0$
$S_{org} = .09$	$k_{rgro} = .7$
$S_{gc} = .05$	
$S_{gr} = .05$	$n_w = 3$
	$n_{ow} = n_{og} = 1.5$
	$n_g = 1.2$

Injection Data

Air injection rate = 190.48 MSCF/D
 at 100°F and 200 psia
 Productivity index = 945 RB-cp/D-PSI

r	Reaction	H_r	E_r	Rate Constant, $A_r \times 10^{-6}$
1	HO + 37.5 O2 → 25 CO2 + 25 H2O	7×10^6	18500	1.0
2	LO + 15.5 O2 → 10 CO2 + 11 H2O	2.846×10^6	18500	1.0
3	HO → 2 LO + 5 COKE	20000	16000	.3
4	COKE + 1.6 O2 → CO2 + 1.2 H2O	$.225 \times 10^6$	13000	1.0

* See reference 4 for the analytical relative permeability expressions.

TABLE 2

EFFECTS OF GRID SIZE ON STB OF HEAVY AND LIGHT OIL BURNED, CRACKED AND PRODUCED

ID RUNS	RUN AX, FT.		
	1 10	1A 10	2 2.5
HO PRODUCED	3320	3334	3724
LO PRODUCED	775	755	336
HO BURNED	300	360	387
HO CRACKED	779	770	337
LO BURNED	9	20	3

TABLE 3

EFFECTS OF GRID SIZE ON STB OF HEAVY AND LIGHT OIL BURNED, CRACKED AND PRODUCED

2D CROSS-SECTION RUNS

RUN GRID	2D CROSS-SECTION RUNS		
	5 5 x 3	6 10 x 3	7 20 x 3
HO PRODUCED	5728	5822	5740
LO PRODUCED	1884	1678	1857
HO BURNED	1175	1333	1283
HO CRACKED	2024	1771	1905
LO BURNED	153	105	60
INJECTOR TPEAK, °F(DAYS)	574(115)	632(78)	753(24.1)
PRODUCER TPEAK, °F(DAYS)	455(560)	579(514)	574(500)

TABLE 4

EFFECTS OF GRID SIZE AND ORIENTATION ON 3-DIMENSIONAL PATTERN 2D AREAL RUN RES. - 5

$T_{ACT} = 400^\circ F$ TIME = 3500 DAYS 9-POINT SCHEME:

RUN GRID	PATTERN 2D AREAL RUN RES. - 5			
	8 5 x 5	9 7 x 4	10 8 x 8	11 11 x 6
HO PRODUCED*	138,500	123,800	114,500	123,100
LO PRODUCED	81,110	92,290	99,260	81,430
HO BURNED	86,820	81,550	78,830	84,930
HO CRACKED	102,100	110,300	114,900	99,270
LO BURNED	13,080	11,690	11,260	11,890
INJECTOR TPEAK, °F(DAYS)	663(90)	637(82)	733(28)	740(27)
PRODUCER TPEAK, °F(DAYS)	323(3000)	423(1840)	371(3000)	357(2783)

* All oil units are STB.

12247

FIGURE 1

MOL FRACTION OXYGEN IN PRODUCED GAS

ID RUN	$\Delta X, FT.$
—	1 10
- - -	2 2.5
o o o	3 .5
$\Delta \Delta$	1A 10 ($T_{ACT} = 400^\circ F$)

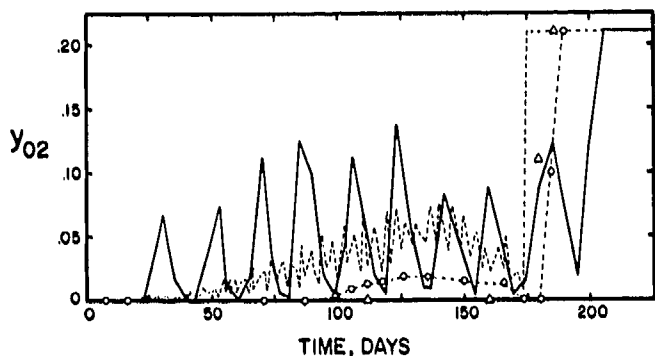


FIGURE 2

CALCULATED OIL RECOVERY VS. TIME

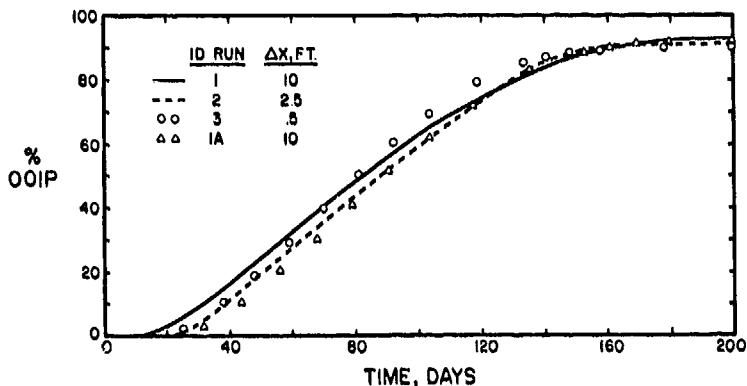


FIGURE 3

EFFECTS OF GRID SIZE AND T_{ACT} ON PEAK TEMPERATURE PROFILES

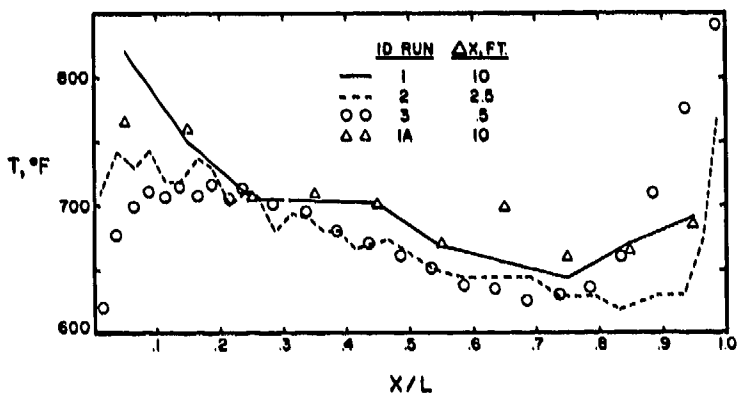


FIGURE 4

OIL RECOVERY VS. TIME FOR 200' x 21' CROSS-SECTION RUNS

RUN	GRID	$\Delta X, FT.$
—	5 x 3	40
- - -	10 x 3	20
o o	20 x 3	10

($T_{ACT} = 400^\circ F$)

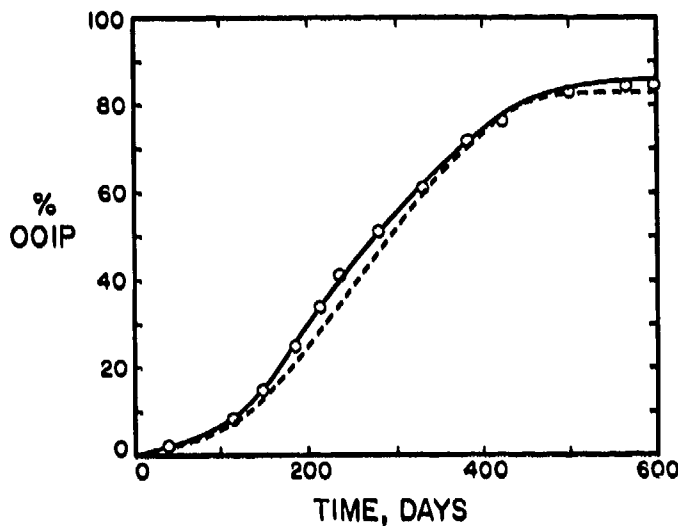


FIGURE 5

TEMPERATURE AND BURNED ZONE PROFILES AT 400 DAYS

RUN 7 20 x 3 CROSS-SECTION

$T_{ACT} = 400^\circ F$

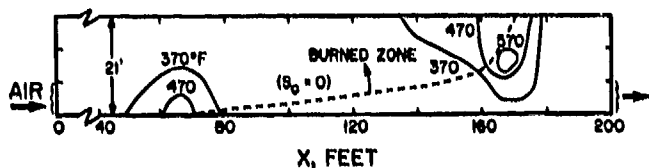


FIGURE 6

GRID ORIENTATION AND GRID EFFECTS ON OIL RECOVERY FOR 20-ACRE 5-SPOT RUNS

RUN	GRID
△ △ 9	7 x 4 PAR.
• • 10	8 x 8 DIAG.
○ ○ 11	11 x 6 PAR.

$T_{ACT} = 400^{\circ}F$ 9-POINT SCHEME

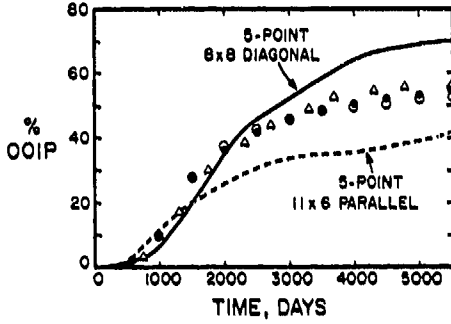


FIGURE 7

CALCULATED TEMPERATURE, SATURATION AND LO MOL FRACTION PROFILES, ID COMBUSTION RUN 4

TIME = 15.75 DAYS $\Delta X = 1.25$ FT.

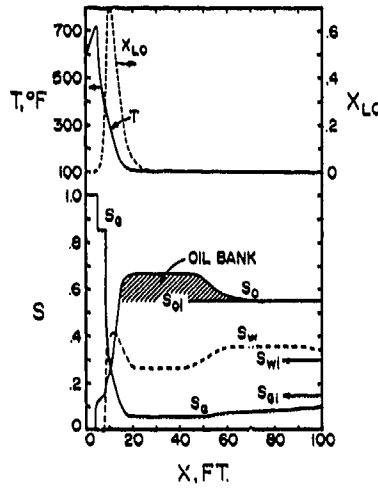


FIGURE 8

EFFECTS OF GRID SIZE ON TEMPERATURE, SATURATION AND LO MOL FRACTION PROFILES

TIME = 23 DAYS

— $\Delta X = 2.5$ FT. (RUN 2)
 - - - $\Delta X = 0.5$ FT. (RUN 3)

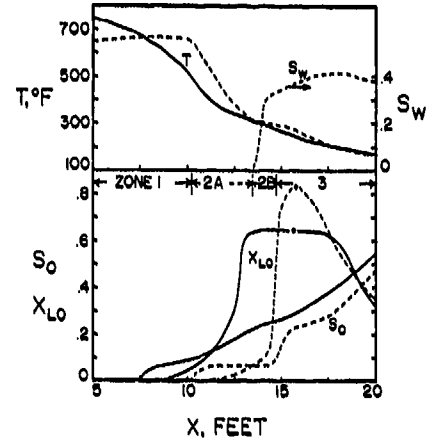


FIGURE 9

THE DISTILLATION EFFECT: PEAK LO MOL FRACTION VS. DISTANCE

$\Delta X, FT.$	RUN
○ ○	5
• •	125
- - -	2.5
△ △	10

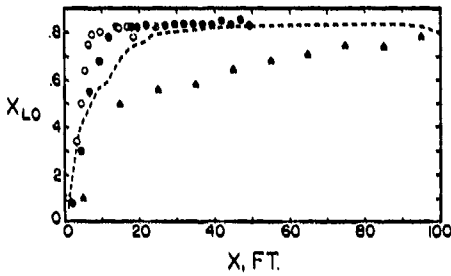


FIGURE 10

HEAVY OIL BURNED, MASS/BULK VOLUME VS. DISTANCE

$\Delta X, FT.$	RUN
○ ○	.5
- - -	2.5
△ △	10

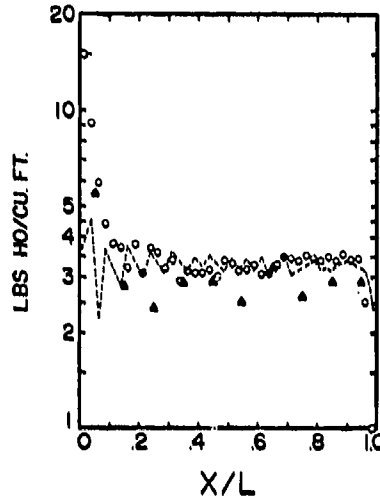


FIGURE 11

HEAVY OIL CRACKED, MASS/BULK VOLUME VS. DISTANCE

$\Delta X, FT.$	RUN
○ ○	.5
- - -	2.5
△ △	10

